



**HAL**  
open science

## Hydrophobic Hydrogels with Fruit-Like Structure and Functions

Hui Guo, Tasuku Nakajima, Dominique Hourdet, Alba Marcellan, Creton Costantino, Wei Hong, Takayuki Kurokawa, Jian Ping Gong

► **To cite this version:**

Hui Guo, Tasuku Nakajima, Dominique Hourdet, Alba Marcellan, Creton Costantino, et al.. Hydrophobic Hydrogels with Fruit-Like Structure and Functions. *Advanced Materials*, 2019, 31 (25), pp.1900702. 10.1002/adma.201900702 . hal-02393171

**HAL Id: hal-02393171**

**<https://hal.science/hal-02393171>**

Submitted on 4 Dec 2019

**HAL** is a multi-disciplinary open access archive for the deposit and dissemination of scientific research documents, whether they are published or not. The documents may come from teaching and research institutions in France or abroad, or from public or private research centers.

L'archive ouverte pluridisciplinaire **HAL**, est destinée au dépôt et à la diffusion de documents scientifiques de niveau recherche, publiés ou non, émanant des établissements d'enseignement et de recherche français ou étrangers, des laboratoires publics ou privés.

# Hydrophobic Hydrogels with Fruit-Like Structure and Functions

Hui Guo, Tasuku Nakajima, Dominique Hourdet, Alba Marcellan, Costantino Creton, Wei Hong, Takayuki Kurokawa, and Jian Ping Gong\*

Normally, a polymer network swells in a good solvent to form a gel but the gel shrinks in a poor solvent. Here, an abnormal phenomenon is reported: some hydrophobic gels significantly swell in water, reaching water content as high as 99.6 wt%. Such abnormal swelling behaviors in the nonsolvent water are observed universally for various hydrophobic organogels containing omniphilic organic solvents that have a higher affinity to water than to the hydrophobic polymers. The formation of a semipermeable skin layer due to rapid phase separation, and the asymmetric diffusion of water molecules into the gel driven by the high osmotic pressure of the organic solvent–water mixing, are found to be the reasons. As a result, the hydrophobic hydrogels have a fruit-like structure, consisting of hydrophobic skin and water-trapped micropores, to display various unique properties, such as significantly enhanced strength, surface hydrophobicity, and antidrying, despite their extremely high water content. Furthermore, the hydrophobic hydrogels exhibit selective water absorption from concentrated saline solutions and rapid water release at a small pressure like squeezing juices from fruits. These novel functions of hydrophobic hydrogels will find promising applications, e.g., as materials that can automatically take the fresh water from seawater.

Polymer gels are defined as crosslinked polymer networks that are swollen in solvents. Since the last three decades, gels, especially water-based hydrogels, have embraced increasing interest for the numerous engineering and biological applications, including bioengineering,<sup>[1,2]</sup> adhesion,<sup>[3,4]</sup> soft robotics,<sup>[5]</sup> and 3D printing.<sup>[6]</sup> Ordinarily, a polymer network swells in a good solvent having a high affinity to polymer, forming a gel. When

experiencing solvent exchange from good to poor, a gel usually exhibits a monotonous deswelling with time if the good and poor solvents are miscible.<sup>[7–11]</sup> During this process, the good solvent easily escapes from gels driven by osmotic pressure of solvent–solvent mixing, while the poor solvent hardly enters the gel due to the demixing of polymer and poor solvent (Figure 1a). Here, we report an abnormal swelling of hydrophobic gels in water to form “hydrophobic hydrogels.” We discovered that when hydrophobic gels swollen with omniphilic organic solvents are immersed in water or aqueous solutions, instead of shrinkage, the hydrophobic gels substantially swell to reach a water content as high as 99.6 wt% at most. The significant swelling of hydrophobic gels in water leads to the formation of a novel class of “hydrophobic hydrogels” that have a unique fruit-like structure and show unique functions such as selective water absorption. To our knowledge, such abnormal swelling phenomenon of hydrophobic gels in water has

never been reported before. This abnormal swelling is attributed to the rapid formation of a semipermeable skin layer on the surface of the gel by the phase separation of the hydrophobic polymer in water, which brings about a strongly asymmetrical diffusion for the organic solvent and water. The impermeable organic solvent is effectively trapped inside the gel, and thus generates a high osmotic pressure which drives the permeable

Dr. H. Guo, Prof. T. Nakajima, Prof. T. Kurokawa, Prof. J. P. Gong  
Laboratory of Soft & Wet Matter  
Faculty of Advanced Life Science  
Hokkaido University  
N21W11, Kita-ku, Sapporo, Hokkaido 001-0021, Japan  
E-mail: gong@sci.hokudai.ac.jp

Dr. H. Guo, Prof. T. Nakajima, Prof. D. Hourdet, Prof. A. Marcellan,  
Prof. C. Creton, Prof. W. Hong, Prof. T. Kurokawa, Prof. J. P. Gong  
Global Station for Soft Matter  
Global Institution for Collaborative Research and Education (GI-CoRE)  
Hokkaido University  
N21W11, Kita-ku, Sapporo, Hokkaido 001-0021, Japan

Prof. T. Nakajima, Prof. J. P. Gong  
Institute for Chemical Reaction Design and Discovery (WPI-ICReDD)  
Hokkaido University  
N21W10, Kita-ku, Sapporo, Hokkaido 001-0021, Japan

Prof. D. Hourdet, Prof. A. Marcellan, Prof. C. Creton  
Laboratoire Sciences et Ingénierie de la Matière Molle  
ESPCI Paris  
PSL University  
Sorbonne Université  
CNRS  
F-75005 Paris, France

Prof. W. Hong  
Department of Mechanics and Aerospace Engineering  
Southern University of Science and Technology  
Shenzhen, Guangdong 518055, P.R. China

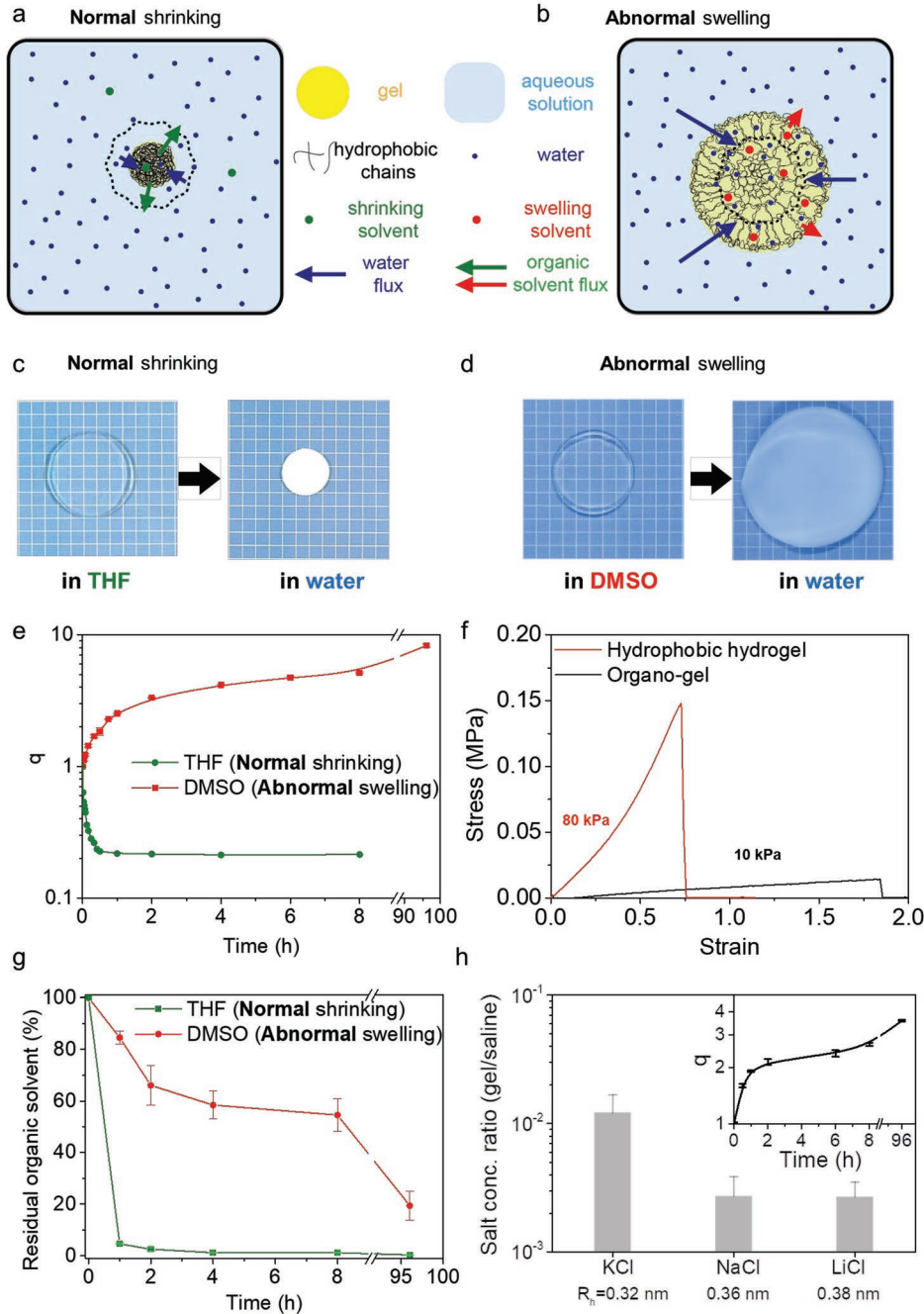


**Figure 1.** Schematic illustration of organogels' volume change upon solvent exchange and the formation of "hydrophobic hydrogels." When organogels constructed from hydrophobic network preswelled in an omniphilic organic solvent are immersed in water, phase separation occurs. Depending on the relative affinity of the organic solvent to the polymer and water, normal shrinking (a) or abnormal swelling (b) of the organogel in water occurs (the dashed line in the figures illustrates the initial size of organogels). In the normal case, the diffusion of the organic solvent and water leads to gel shrinking due to phase separation. In the abnormal case, robust phase separation results in the formation of semipermeable structure to trap the organic solvent inside the gel. As a result, the gel substantially swells by the high osmotic pressure of the organic solvent. c) Photograph of normal shrinking: PMA organogel at equilibrium state in THF (left) and after immersing PMA-THF organogel in water for 8 h at 25 °C. d) Photograph of abnormal swelling: PMA organogel at equilibrium state in DMSO (left) and after immersing PMA-DMSO organogel in water (right) for 8 h at 25 °C. e) Time profiles of swelling ratio ( $q$ ) of PMA organogels from THF and DMSO after being immersed in water at 25 °C. The initial size of the disc shape samples was 35 mm in diameter and 2 mm in thickness. f) Uniaxial tensile behaviors of the PMA-DMSO organogel (d, left) and its PMA hydrogel (d, right). The Young's moduli of the two gels are shown beside the curves. g) Time profiles of the residual organic solvent in the PMA organogels after being immersed in water. The residual organic solvent ratio is defined as the amount of organic solvent relative to the initial state. h) Salt concentrations inside PMA hydrogels over that in saline solution after being swelled in saline solutions (10 wt%) for 4 d at 25 °C. The hydrated radii ( $R_h$ ) of cations are illustrated below the columns, noting that the cations have bigger radii than the anion. The inserting figure shows the time profile of swelling ratio ( $q$ ) of the gel in 10 wt% (1.7 M) NaCl solution.

water to diffuse into the gel robustly. The water absorption of the hydrophobic gels causes phase separation to form porous structure inside the gels (Figure 1b).

As an example, we first show the different swelling behaviors of hydrophobic poly(methyl acrylate) (PMA) gels containing two different omniphilic organic solvents, tetrahydrofuran (THF) and dimethylsulfoxide (DMSO) (Figure 1c,d). The covalently crosslinked PMA gels were initially prepared in DMSO and subsequently swollen in THF or DMSO until equilibrium. Although the dry PMA network barely swells in water,<sup>[12]</sup> its organic gels exhibit very different behaviors. After being immersed in water, both gels experienced a fast phase separation by water infusion: the originally transparent gels rapidly turned to opaque and then white, starting from surfaces. However, they exhibited striking differences in volume change. The PMA–THF gel monotonically shrank with time, as commonly expected for a swollen gel immersed in a poor solvent that is miscible with the original solvent in the gel (Figure 1c,e; Video S1, Supporting Information). After 30 min, the PMA–THF gel shrank to only 20% of its initial size in water. In contrast, the PMA–DMSO gel surprisingly increased its volume rapidly with time in water, indicating that a large amount of water was absorbed by the hydrophobic PMA gel (Figure 1d,e; Video S2, Supporting Information). After 8 h, the volume of the gel boosted more than five times of its initial value in DMSO, and the water content reached a level as high as 99 wt%. The abnormal swelling in water is reversible, and it can be repeated by cyclically exchanging the solvent from DMSO to water for many times (Figure S1, Supporting Information). The organogels always exhibit swelling performance after immersion in water. However, the swelling ratio of the gels in water gradually decreases with the increase of the cycle number, especially at the second cycle, probably due to some damage of the pristine sample upon the significant swelling in the first cycle. Interestingly, while the DMSO-swollen PMA gel is soft and showing a mechanical response typical of rubbery materials (Figure 1f), the gel becomes much stiffer and stronger after significant swelling in water. The strengthening of the hydrophobic hydrogel can be attributed to the strain-hardening of the polymer chains induced by remarkable volume expansion as well as the mesoscale aggregated structure formed by phase separation.<sup>[10,13]</sup>

It is well established that, the swelling of a polymer network in a good solvent is driven by the gain in the free energy of mixing between the polymer and the solvent, and a swelling equilibrium is reached when this mixing energy gain is counterbalanced by the elastic energy of the polymer chains. In a poor solvent, the polymer and the solvent phase separate and the equilibrium swelling dramatically decreases. Therefore, the observed swelling of PMA–DMSO gel in water that is a poor solvent of the PMA cannot be explained by this thermodynamic equilibrium theory. To reveal the driving force for the absorption of water into the hydrophobic PMA network, we analyzed the amount of organic solvent in the gels as a function of swelling time. As shown in Figure 1g, the amount of THF in the gels decreased rapidly: only about 1% of THF relative to the initial amount remained in the gel after 4 h of immersion in water. However, the amount of DMSO maintained an elevated level and about 20% of DMSO still remained in the gel even after 4 d despite the frequent refreshing of the water bath. Since both organic solvents are completely water miscible, the

significant difference in the amount of residual organic solvents brings about a huge difference in osmotic pressure. That is, for the THF-swollen PMA gel, the negligible amount of THF in the PMA gel contributes insignificantly to balance the desolvation of the hydrophobic PMA in water, thus the gel shrank. In contrast, the large amount of remaining DMSO generates a large osmotic pressure to imbibe the water and swell the gel, as like the effect of counterions on the swelling of polyelectrolyte gels. This osmosis-driven swelling is further confirmed by immersing the PMA–DMSO gel in various aqueous solutions containing DMSO to increase the osmotic pressure of the bath solution. The gels exhibited a lower swelling capability at a higher DMSO concentration aqueous solution (Figure S2, Supporting Information), which confirms the osmosis effect.

The extremely low release rate of DMSO implies that a semipermeable structure, easily permeable to water but hardly to DMSO, is formed on the surface of the gel with the polymer phase separation, which leads to the asymmetric diffusion. In fact, without polymer phase separation, a hydrophilic poly(hydroxyethylacrylate) (PHEA) gel swollen in DMSO lost the organic solvent readily in water (Figure S3, Supporting Information).

The PMA–DMSO gel also swells in saline solution, and the semipermeable skin layer is hardly permeable to ions. In 10 wt% alkali chloride salt solutions, the gel still attains a swelling around four times by volume regardless of the high osmotic pressure of the saline solution (Figure 1h, insert). The concentration of ions inside the swollen hydrophobic hydrogel is only 0.1–1% of that in the bath solutions, displaying a slightly higher selectivity to Na<sup>+</sup> and Li<sup>+</sup> ions having larger hydrodynamic radius  $R_h$  than to K<sup>+</sup> ion (Figure 1h). These results support the hypothesis of a semipermeable structure formation: the hydrated ions, which have much larger radii than water, can hardly pass through the semipermeable structure. Accordingly, the phase separation induces a condensed polymer structure to show the semipermeable effect. When certain amount of defects was introduced into the membranes by copolymerization of hydrophilic segments with the hydrophobic MA, the swelling of the gel in water was suppressed, although the relative hydrophilicity of the gel was increased (Figure S4, Supporting Information).

Why was the semipermeable skin layer formed in the DMSO gel but not in the THF gel that also exhibited a phase separation? Or more generally, what is the general requirement on the organic solvents to show the abnormal swelling phenomenon? To answer these questions, we further investigated the behavior of the PMA gels in six other omniphilic organic solvents, and the results are shown in Figure 2a. The PMA gels preswelled in DMF (*N,N*-dimethylformamide), NMP (*N*-methyl-2-pyrrolidone), DMAc (*N,N*-dimethylacetamide), or NMF (*N*-methylformamide) showed a significant swelling in water, similar to the behavior observed for DMSO. In contrast, the PMA gels preswelled in acetone and MeCN (acetonitrile) shrank in water, as was the case for THF. Among the different samples tested, the maximum swelling ratio, which was attained by the PMA–DMAc gel, reached about two orders of magnitude higher than PMA–THF or PMA–MeCN. In agreement with the results shown in Figure

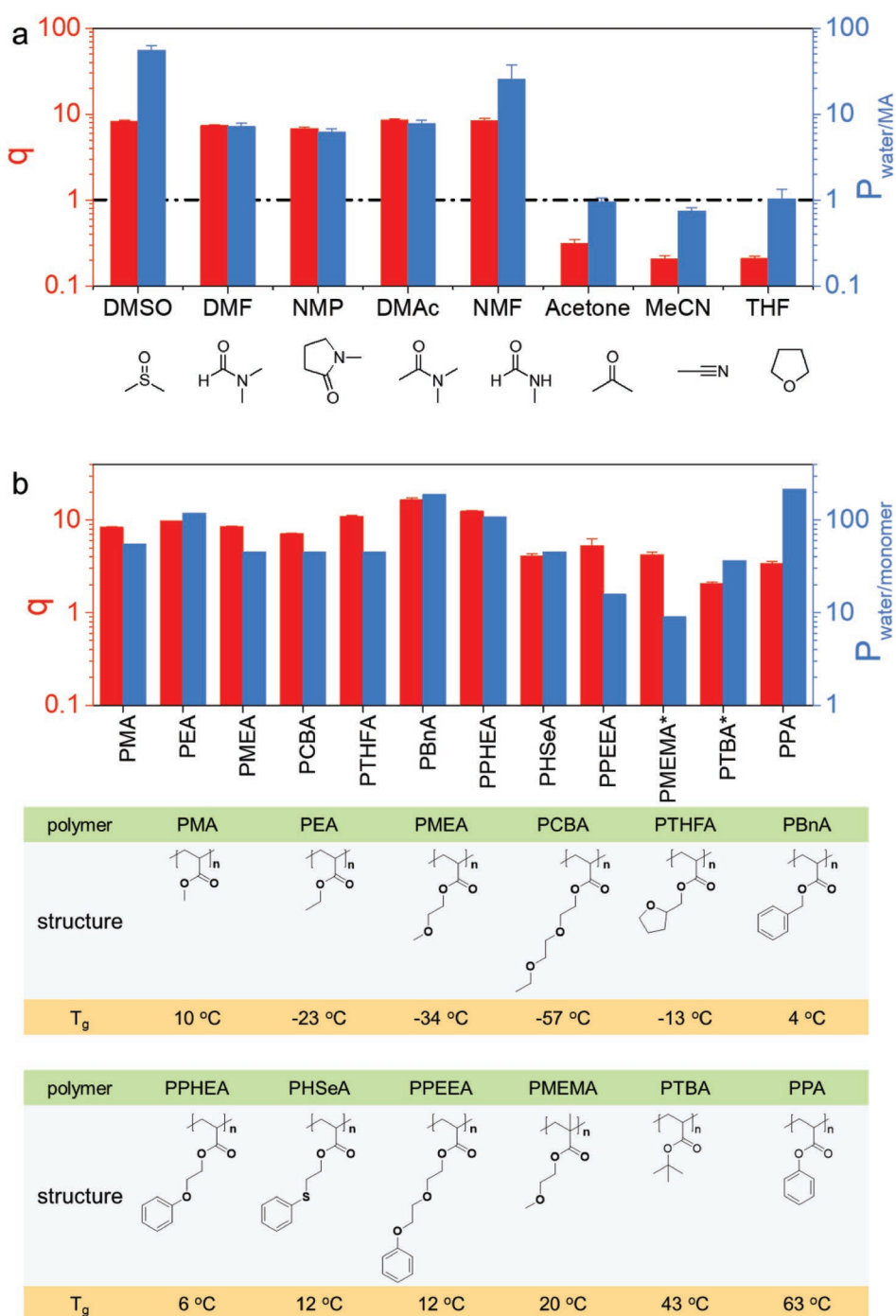


**Figure 2.** Generalization of the abnormal swelling of organogels in water. a) Solvent effect. Red column: maximum swelling ratio ( $q$ ) of PMA gels starting from organogels in different solvents at 25 °C; blue column: partition coefficient ( $P_{\text{water/MA}}$ ) of different organic solvents in water over that in MA.  $q = 1$  means that the gels volume remains unchanged, and  $P_{\text{water/MA}} = 1$  means that the organic solvents have the same affinity to water and MA (guided as dash line). Chemical structures of solvents are illustrated below the figure. All the organogels were initially synthesized in DMSO and immersed in different solvents until equilibrium state. b) Polymer effect. Red column: maximum swelling ratio of different organogels in water at 25 °C. The organogels were preswelled in DMSO (except for PMEMA and PTBA, which were preswelled in DMF). Blue column: partition coefficient ( $P_{\text{water/monomer}}$ ) of DMSO in water over that in different monomers (in the cases of PMEMA and PTBA, DMF was used in the place of DMSO). Chemical structures of polymers and glass transition temperature ( $T_g$ ) of the linear polymers are illustrated below the figure.

into two categories: “swelling solvents,” such as DMSO, DMF, NMP, DMAc, and NMF; and “shrinking solvents,” such as THF, acetone, and MeCN. While all these organic solvents have

comparable physical properties (e.g., molecular size, dielectric constant, solubility parameter), their relative affinities to water and polymer are remarkably different, as measured by the

partition-coefficient test (Figure 2a). All the “swelling solvents” have much stronger affinities to water than to the monomer MA ( $P_{\text{water/MA}} \gg 1$ ), while all “shrinking solvents” display comparable affinities between water and MA ( $P_{\text{water/MA}} \approx 1$ ). These results agree with the mixing enthalpy of the organic solvent and water. That is, the “swelling solvents” have much higher affinity to water than “shrinking solvents.”<sup>[14–19]</sup> Meanwhile, all the solvents investigated show no significant difference in their affinity to the PMA network, as seen from the comparable equilibrium swelling ratio of PMA gels in these solvents (Figure S5b, Supporting Information).

To clarify the universality of this abnormal swelling phenomenon, we further studied the swelling behavior of 11 organogels from different hydrophobic polymers. These gels were initially swollen in “swelling solvent” DMSO or DMF. As shown by the partition coefficient  $P_{\text{water/monomer}}$  in Figure 2b, the affinity of the organic solvents to water is always higher than the corresponding monomers of these 11 gels. All of these organogels displayed swelling in water, as like the PMA organogel, and the highest water content reached 99.6% for poly(benzyl acrylate) (PBnA). The above results show that the abnormal swelling is a general phenomenon for a hydrophobic network preswollen in an organic solvent that has a higher affinity to water than to the polymer segment.

While all these hydrophobic organogels exhibited swelling in water, the long-time swelling profiles varied with the relationship between the swelling temperature ( $T_{\text{obs}}$ ) and the glass transition temperature ( $T_g$ ) of the polymer (Figure S6a, Supporting Information). The gels from PMA polymers with  $T_g < T_{\text{obs}}$  (room temperature) swelled in water and reached their maximum volume after several days, and then gradually decreased in volume at a quite low rate, exhibiting no swelling equilibrium. By contrast, the gels from poly(phenyl acrylate) (PPA) polymers with  $T_g > T_{\text{obs}}$  exhibited an equilibrium swelling but with a relatively low swelling ratio at equilibrium. We consider that the deswelling at the long-time scale for polymers with  $T_g < T_{\text{obs}}$  is due to the continuous leakage of the organic solvent, which reduces the osmotic pressure. As the swelling is controlled by the competition between the osmotic pressure of the trapped organic solvent and the contractile elasticity of the gel, the leakage of the organic solvent reduces the osmotic pressure and results in the deswelling at long time scale. On the other hand, the less swelling ability and swelling saturation for polymers with  $T_g > T_{\text{obs}}$  can be attributed to the plasticity of the phase separation structure during swelling, which increases the swelling resistance but diminishes the contractile elasticity. As a result, the gel maintained a constant volume even when all of the organic solvents diffused out of the gel (Figure S6b, Supporting Information). After a prolonged time in water, we can obtain highly swollen hydrophobic hydrogels with negligible amount of residual organic solvent.

To reveal the structure evolution during the abnormal swelling of the hydrophobic gel in water, we observe the cross-section of the disc-shape samples through the thickness direction (Figure 3a, upper). Figure 3b,c show the observation on a PMA–DMSO gel (initial diameter  $d = 35$  mm and thickness  $t = 2$  mm) swollen in water for 8 h. Under polarized optical microscopy, a strong birefringence is observed in the outer layer near surface of several hundreds of microns, indicating that orientated structure is formed near the surface

(Figure 3b). Laser microscopy observation further reveals that the oriented structure is attributed to an elongated morphology aligned vertical to the surface plane (Figure 3c). Beneath this vertically aligned layer, an isotropic layer containing large bubbles is observed. Close to the center of the sample, a relatively smooth morphology with small bubbles aligned slightly parallel to the surface is observed. The elongated outer layer starts to form around 0.5 h, becomes thicker with time, and then blurs to show an obscure boundary between different layers (Figure S7a, Supporting Information). At 4 d when the swelling ratio reaches the maximum, the center layer completely disappears to show isotropic morphology. After that, the gel keeps the isotropic morphology during the slow deswelling process. The layered morphology formed during the swelling process reveals the kinetics of water diffusion during the solvent exchange process. At the early stage, the outer layer near surface swells while the inner layer is unswollen, which generates an internal stress mismatching. As a result, the swollen outer layers receive a compression from the unswollen inner layer, leading to the elongated shape of outer layer aligned vertically to the surface, as shown by Figure 3b,c. In turn, the inner layer receives a tension from the swollen outer layer to show slight orientation parallel to the surface.

In order to clarify the microstructure, we performed scanning electron microscopy (SEM) observation of a PPA hydrogel after freeze-drying. The high  $T_g$  of PPA (63 °C) can maintain the structure after dehydration of the hydrophobic hydrogel, which makes it suitable for structure observation. SEM images reveal that the outermost surface of the sample is covered by a thin dense layer which is a few micrometers thick (Figure 3d). Beneath this dense skin layer, a porous layer with slight anisotropy aligned vertical to the surface, of hundred micrometer thickness, is observed. The dense surface layer is the strong evidence of the semipermeable skin layer, while the anisotropic porous layer well corresponds to the swelling outer layer revealed by the optical observation (Figure 3a, lower).

For a ternary system composed of polymer, good solvent, and poor solvent in which the two solvents are miscible, it has been reported that instantaneous demixing occurs when the good solvent has a high affinity to the poor solvent, and a structure composed of a dense skin layer of several  $\mu\text{m}$  thickness and oriented porous layer of hundred  $\mu\text{m}$  thickness aligned vertical to the surface is formed for a polymer membrane.<sup>[20–23]</sup> On the other hand, delayed demixing occurs when the good solvent has a low affinity to the poor solvent, and open porous structure is formed. Here, similar thing happens. When immersing the hydrophobic organogel in water, the “swelling solvents” induce instantaneous demixing to form a condensed semipermeable membrane on the gel surface. At molecular level, these “swelling solvents” have larger size than water. Moreover, the strong interaction between the “swelling solvents” and water results in plausible clusters. Once the clusters are formed, the “swelling solvents” are further immobilized and the size discrimination between DMSO/water cluster and water molecular is more remarkable, therefore these organic solvents diffuse much slower than water across the membrane. In contrast, the “shrinking solvents” results in delayed demixing to form open porous structure, which releases the organic solvent quickly.

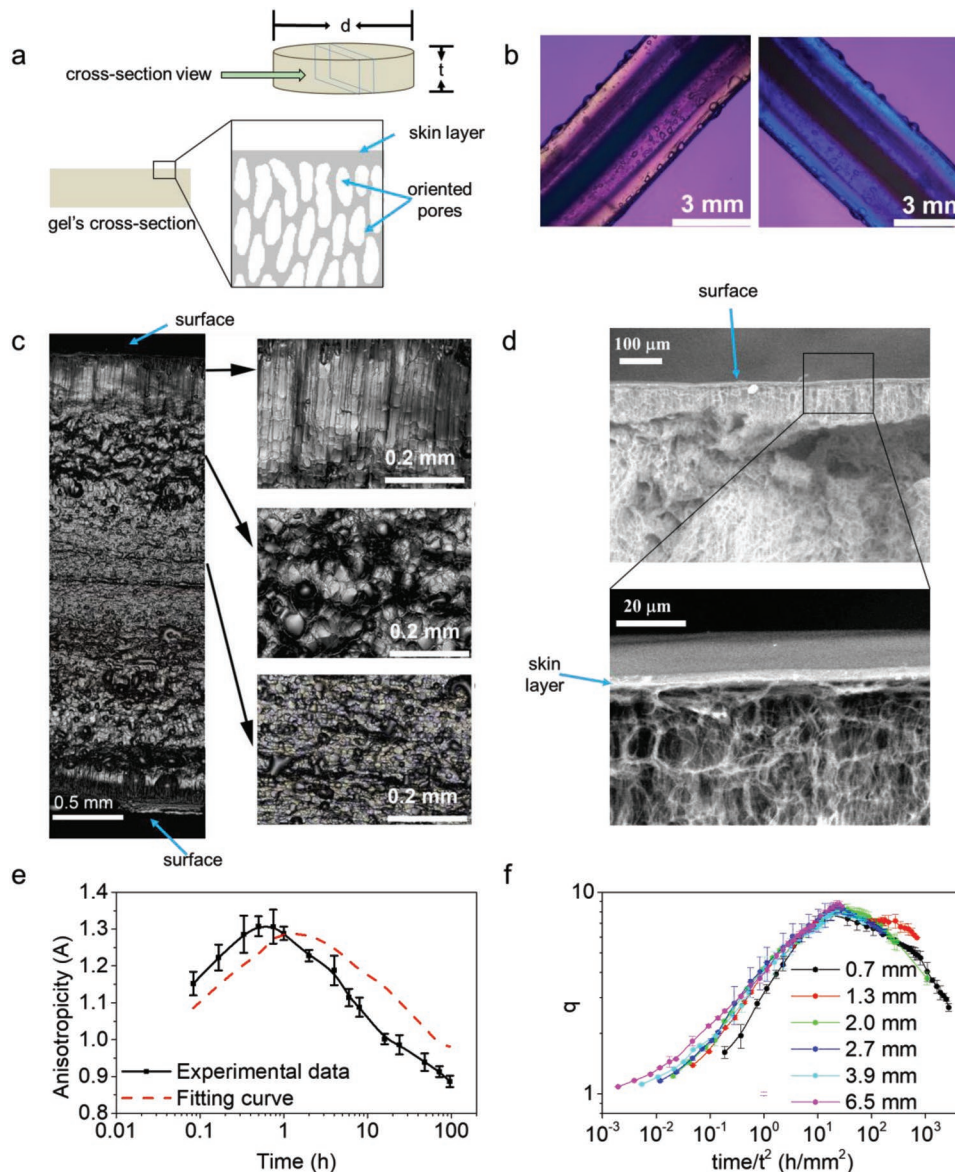


**Figure 3.** Structure analysis and anisotropic swelling kinetics of PMA–DMSO gels in water. a) Dimension of disc-shape gel used for swelling and structure observation (upper) and illustration of the skin layer and oriented porous structure revealed by the structure analysis (lower). b) Polarized optical microscopy images of sample' fresh cut cross-section perpendicular to the disc surface at  $+45^\circ$  and  $-45^\circ$  rotation with the 532 nm sensitive tint plate. c) 3D laser microscopy images of the fresh cut cross-section of hydrophobic hydrogel during swelling. The samples in (b,c) were obtained by immersing the organogel ( $d = 35$  mm diameter,  $t = 2.0$  mm thickness) in water for 8 h at  $25^\circ\text{C}$  and then cutting a slab ( $\approx 1$  mm thickness). d) SEM cross-section view of a PPA–DMSO gel swelled in water for 40 d. The zoomed-in image clearly shows that a dense skin layer of  $\approx 100$   $\mu\text{m}$  is formed on the top of the porous surface layer. e) Swelling anisotropy of discoid organogel in water. The swelling anisotropy ( $A$ ) is the swelling ratio of the diameter divided by that of the thickness ( $A = (d'/d)/(t'/t)$ ). The red-dashed curve was obtained from a “sandwich structure” model using proper fitting parameters (see the Supporting Information). f) Size dependence of swelling kinetics at  $25^\circ\text{C}$ : master curve of swelling kinetics of discoid organogels with different initial thickness  $t$  while the initial diameters  $d$  of the gels was fixed at 35 mm.

Due to the formation of the layered structure, swelling kinetics of the hydrophobic gels in water is anisotropic. For a disc-shaped sample of diameter  $d = 35$  mm and thickness  $t = 2$  mm, the degree of anisotropy  $A$ , defined as the ratio of relative size change in diameter to thickness,  $A = (d'/d)/(t'/t)$ , first increases to 1.3 and then gradually decreases to a value near 1 (Figure 3e). This indicates that the diameter increases faster than the thickness ( $d'/d > t'/t$ ) at the initial swelling stage, which is opposite to that for

normal swelling of a gel in good solvents. This is because the outer swollen layer with elongated pore structure is stiffer than the inner unswollen layer, as revealed in Figure 1f, therefore the inner layer is more prone to deform to show anisotropic swelling. Using a simple “sandwich structure” model (Supporting Information), in which the two outer layers are more rigid and swollen than the middle inner layer, and the outer layers become thick with time, the time profile of the experimental swelling

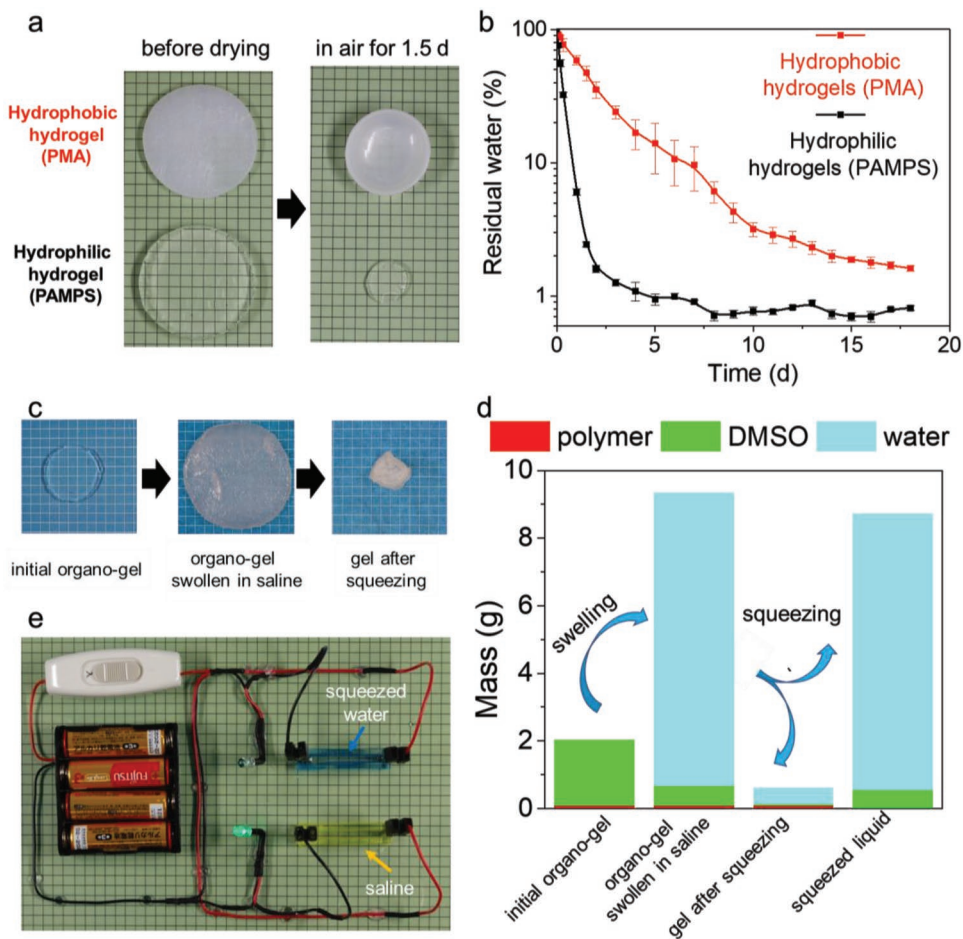


**Figure 4.** Demonstration of water retention, desalination, and recovery. a) Images to show the difference of water retention capacity between a hydrophobic PMA hydrogel and a hydrophilic poly(2-acrylamido-2-methyl-1-propanesulfonic acid) (PAMPS) hydrogel at 25 °C. Both hydrogels have the same initial size ( $d = 50$  mm,  $t = 4$  mm) and comparable water content (99 wt%). b) Retained water ratio of a hydrophobic PMA hydrogel and a hydrophilic PAMPS hydrogel at 25 °C in fume hood (humidity: 40%). c) Photos of the organogel at initial state, organogel swollen in saline solution (NaCl, 3 wt%) for 48 h, and the gel after being compressed with normal compressive stress  $\approx 0.5$  MPa for 2 s. d) Compositions of the initial organogel, the gel after swollen in saline, the gel after squeezing, and the squeezed liquid. Note that the salt in the swollen gels and squeezed liquid could not be detected within the experimental accuracy, indicating a high selectivity to water absorption. e) Photograph demonstrating the low salt content in the squeezed liquid from the hydrophobic hydrogel. The swelling media (NaCl saline, 3 wt%, yellow channel) has a high electric conductivity to light the bulb while the squeezed liquid from the hydrophobic hydrogel (blue channel) could not be due to low conductivity.

anisotropy are reproduced satisfactorily (Figure 3e, dash line). In addition, the “sandwich” model also reproduces the time evolution of the fraction of swollen outer layers relative to the whole sample thickness (Figure S7c, Supporting Information).

To study the effect of the semipermeable skin layer on the abnormal swelling, we further carried out the swelling experiment in water with disc-shape PMA organogels of constant diameter ( $d = 35$  mm) but different thicknesses ( $t = 0.7$ – $6.5$  mm). The time profiles of the swelling ratio are depicted in Figure 3f, in which the swelling time is normalized by the square of the initial sample thickness ( $\text{time}/t^2$ ). During the swelling process, thinner sample shows a smaller swelling than the thick sample for the same normalized time, while the maximum swelling ratio and the deswelling kinetics collapsed to a master curve. These results indicate that the maximum swelling ratio is independent of thickness, while the time to reach the maximum swelling increases with the square of thickness. The systematic

deviation of swelling ratio to smaller value for thinner sample in the master curve indicates the effect of the surface skin layer. Since the thickness of the skin layer is independent of the total sample thickness, the thickness fraction of skin layer increases with the decrease of the sample thickness, leading to more retardation effect to swelling ratio. On the contrary, the collapse of the kinetic profiles in the deswelling process features a simple diffusion in a homogeneous gel, which well agrees with the structure observation (Figure S7a, Supporting Information).

The above results indicate that when an organogel is immersed in water, a dense skin layer of several micrometer thickness is formed on the surface due to instantaneous demixing of polymer and water. This skin layer serves as a semipermeable membrane to suppress the diffusion of the organic solvent to the bath while the diffusion of water molecules is less affected. As a result, the water molecules diffuse into the gel, driven by the high osmotic pressure generated by



the trapped organic solvent. With the increase of water content inside the gel, local phase separation occurs to form porous structure inside the gel. Due to the large swelling and stiffening of the two outer layers, the gel swells faster in lateral direction, exhibiting an anisotropic swelling.

The hydrophobic hydrogels exhibit various unique functions which may greatly broaden their applications. For example, regardless of the extremely high water content, the PMA hydrogels have a hydrophobic surface, showing a static contact angle of  $92 \pm 3^\circ$  to water (Figure S8, Supporting Information), which is much higher than that of common hydrogels with an equivalent water content.<sup>[24]</sup> Thus, the hydrophobic hydrogels have a structure consisting of a hydrophobic dense skin and micropores containing trapped water, a structure similar to fruits such as an orange. Such structure significantly delays the evaporation of water molecules from the hydrophobic hydrogels in comparison with conventional hydrogels from hydrophilic polymers (Figure 4a). As presented in Figure 4b, a conventional hydrogel from poly(2-acrylamido-2-methyl-1-propanesulfonic acid) (PAMPS) quickly dried in the fume hood within 1 d, whereas the PMA hydrophobic hydrogel stored in the same condition still maintained 10% of water after one week. Moreover, as like a fruit, the water in the hydrophobic gels can be quickly squeezed out with a small pressure (Figure 4c). This is very different from the conventional hydrophilic hydrogels where high pressure and long-time are required to squeeze the water from the hydrogel since water is hydrated with the nanoscale polymer network.<sup>[25]</sup> Combining the previously described property of selective water absorption in saline solutions, the hydrophobic hydrogels are promising materials for energy-free sea water desalination or marine lifesaving. As demonstrated in Figure 4d,e and Video S3 of the Supporting Information, an PMA–DMSO organogel spontaneously absorbs large amount of water from a 3 wt% NaCl saline solution, while leaving nearly all the solutes in the swelling media. Then, with a household squeezer, salt-free water can be easily squeezed out from the gel without breaking the gel.

As the abnormal swelling of hydrophobic gels in water is universal, numerous hydrophobic polymers can be applied to develop water containing materials. The various unique properties of the hydrophobic hydrogels make them as novel promising materials for applications in biomedical, agricultural, and industrial fields.

## Experimental Section

Experimental details are provided in the Supporting Information.

## Supporting Information

Supporting Information is available from the Wiley Online Library or from the author.

## Acknowledgements

This work was supported by JSPS KAKENHI (Grant no. JP17H06144, 17H06376). Institute for Chemical Reaction Design and Discovery (ICReDD) was established by World Premier International Research Initiative (WPI), MEXT, Japan. The authors thank Yoshiyuki Saruwatari of Osaka Organic Chemical Industry Ltd. for the supply of certain

- 
- K. Y. Lee, D. J. Mooney, *Prog. Polym. Sci.* **2012**, *37*, 106.
- [2] M. W. Tibbitt, C. B. Rodell, J. A. Burdick, K. S. Anseth, *Proc. Natl. Acad. Sci. USA* **2015**, *112*, 14444.
- [3] S. Rose, A. PrevotEAU, P. Elziere, D. Hourdet, A. Marcellan, L. Leibler, *Nature* **2014**, *505*, 382.
- [4] J. Li, A. D. Celiz, J. Yang, Q. Yang, I. Wamala, W. Whyte, B. R. Seo, N. V. Vasilyev, J. J. Vlassak, Z. Suo, D. J. Mooney, *Science* **2017**, *357*, 378.
- [5] C. Yang, Z. Suo, *Nat. Rev. Mater.* **2018**, *3*, 125.
- [6] Y. Kim, H. Yuk, R. Zhao, S. A. Chester, X. Zhao, *Nature* **2018**, *558*, 274.
- [7] S. Abdurrahmanoglu, V. Can, O. Okay, *Polymer* **2009**, *50*, 5449.
- [8] H. Guo, N. Sanson, D. Hourdet, A. Marcellan, *Adv. Mater.* **2016**, *28*, 5857.
- [9] G. Miquelard-Garnier, S. Demoures, C. Creton, D. Hourdet, *Macromolecules* **2006**, *39*, 8128.
- [10] K. Sato, T. Nakajima, T. Hisamatsu, T. Nonoyama, T. Kurokawa, J. P. Gong, *Adv. Mater.* **2015**, *27*, 6990.
- [11] H. Guo, C. Mussault, A. Marcellan, D. Hourdet, N. Sanson, *Macromol. Rapid Commun.* **2017**, *38*, 1700287.
- [12] A. Shundo, K. Hori, D. P. Penaloza, K. Yoshihiro, M. Annaka, K. Tanaka, *Phys. Chem. Chem. Phys.* **2013**, *15*, 16574.
- [13] H. Kamata, Y. Akagi, Y. Kayasuga-Kariya, U.-i. Chung, T. Sakai, *Science* **2014**, *343*, 873.
- [14] H. L. Clever, S. P. Pigott, *J. Chem. Thermodyn.* **1971**, *3*, 221.
- [15] M. J. Costigan, L. Hodges, K. Marsh, R. Stokes, C. Tuxford, *Aust. J. Chem.* **1980**, *33*, 2103.
- [16] M. Cilense, A. V. Benedetti, D. R. Vollet, *Thermochim. Acta* **1983**, *63*, 151.
- [17] A. V. Benedetti, M. Cilense, D. R. Vollet, R. C. Montone, *Thermochim. Acta* **1983**, *66*, 219.
- [18] K. Morcom, R. Smith, *J. Chem. Thermodyn.* **1969**, *1*, 503.
- [19] S. Murakami, R. Tanaka, R. Fujishiro, *J. Solution Chem.* **1974**, *3*, 71.
- [20] C. Smolders, A. Reuvers, R. Boom, I. Wienk, *J. Membr. Sci.* **1992**, *73*, 259.
- [21] R. Bakhshi, E. Vasheghani-Farahani, H. Mobedi, A. Jamshidi, M. Khakpour, *Polym. Adv. Technol.* **2006**, *17*, 354.
- [22] G. R. Guillen, Y. Pan, M. Li, E. M. V. Hoek, *Ind. Eng. Chem. Res.* **2011**, *50*, 3798.
- [23] W. Lu, Z. Yuan, Y. Zhao, H. Zhang, H. Zhang, X. Li, *Chem. Soc. Rev.* **2017**, *46*, 2199.
- [24] F. J. Holly, M. F. Refojo, in *Hydrogels for Medical and Related Applications* (Ed: J. D. Andrade), American Chemical Society, Washington, DC, USA **1976**, pp. 252–266.
- [25] Y. R. Zhang, K. J. Xu, Y. L. Bai, L. Q. Tang, Z. Y. Jiang, Y. P. Liu, Z. J. Liu, L. C. Zhou, X. F. Zhou, *J. Mech. Behav. Biomed. Mater.* **2018**, *85*, 181.